On the Use of Channel Models and Channel Estimation Techniques for Massive MIMO Systems

Martin Kuerbis*, Naveen Mysore Balasubramanya†, Lutz Lampe† and Alexander Lampe*
*Hochschule Mittweida - University of Applied Sciences, Mittweida, Germany.
†Department of Electrical and Computer Engineering, University of British Columbia, Vancouver, Canada.

***Abstract*—Massive multiple-input multiple-output (MIMO) is a key technology driving the 5G evolution. It relies on the use a large number of antennas at the base-station to improve network performance. The performance of massive MIMO systems is often limited by imperfect channel estimation because of pilot contamination. Recently, several channel estimation techniques have been proposed to minimize the performance degradation. However, the assessment of these techniques in the literature has often been conducted considering standard channel models, like the independent Rayleigh fading model and Clarke's multi-path model, which do not consider spatial correlation. In this work, we investigate different channel models used and proposed for massive MIMO transmission and, through numerical studies, highlight their effect on the performance of the aforementioned channel estimation techniques. Based on this we recommend the use of channel models that capture the spatial correlation between antennas and different user channels.**

I. Introduction

WITH the advancements in antenna technology and enhanced computational capabilities of network components, the deployment of massive multiple-input multiple-output (MIMO) systems has become feasible [1], [2]. These massive MIMO systems, incorporating a large number of antennas at the base-station (BS), have the ability to improve the network capacity by adopting efficient mechanisms for data transmission. Massive MIMO is being considered as a primary candidate for facilitating the Internet-of-Things (IoT), which is the driving force behind the fifth generation (5G) communication technologies.

A key component in the evaluation of a massive MIMO system is the underlying channel model. Most of the research in this field uses standard channel models such as the spatially and temporally independent and identically distributed (i.i.d.) Rayleigh model or Clarke's multi-path model, which only considers temporal correlation. Consequently, these models do not incorporate spatial correlation, which arises due to the limited number of scatterers in the propagation environment and the compact packing of the antenna elements. Practical channel measurements obtained from a massive MIMO measurement campaign show that spatial correlation is significant and is an important factor governing the system performance [3]. Besides the standard models, the correlated Rayleigh channel model, accounting for both spatial and temporal correlation is proposed in [4], and the COST 2100 model, derived from measurements for conventional MIMO systems, is introduced in [5], [6]. Recently, the COST 2100 model is shown to be close to the practical channel measurements obtained by the massive MIMO measurement campaign in [3]. However, its high computational complexity results in increased simulation time for the evaluation of massive MIMO related techniques using this model.

Another important problem to be addressed in massive MIMO systems is pilot contamination, which degrades the channel estimation performance at each BS. This occurs because each cell in the network uses the same set of orthogonal pilot sequences and the number of such sequences is limited. Moreover, the pilot transmission duration cannot exceed the coherence time of the channel being estimated. Therefore, users in neighbouring cells might reuse the same pilot sequences, which causes interference. Hence, channel estimation techniques that can eliminate or minimize pilot contamination are desirable. Though various such channel estimation algorithms have been proposed in the massive MIMO literature, their performance evaluation has been limited to the case of standard channel models and determining their suitability for practical scenarios remains an important problem to be addressed.

In this work, we focus on the performance of three existing channel estimation techniques proposed for massive MIMO systems - pilot sequence hopping with Kalman filtering [7], amplitude/angular based projection [8], [9] and polynomial expansion [10]. We evaluate the performance of the aforementioned techniques for Clarke's model, the correlated Rayleigh and the COST 2100 models. We demonstrate that the blind pilot decontamination technique based on amplitude/angular projection is quite sensitive to the underlying channel model, the Kalman filtering technique shows similar performance for all the three models and the polynomial expansion method gives the best performance.

II. System Model

We consider a cellular wireless communication system consisting of B cells, with one BS per cell. Each BS is equipped with M antennas and serves K autonomous single-antenna user equipment (UE) simultaneously. We assume that the whole system, i.e., all cells and all UEs in each cell, are fully synchronized. Using this model, we describe the channel between the UEs in cell j and the BS in cell b as $\boldsymbol{H}_{bj} \in \mathbb{C}^{M\times K}$. The k-th column of $\boldsymbol{H}_{bj}$, denoted as $\boldsymbol{h}_{bj_k} \in \mathbb{C}^{M\times 1}$ refers to the channel between UE k in cell j and the BS in cell b. The m-th entry of $\boldsymbol{h}_{bj_k}$, denoted as $h_{b_m j_k} \in \mathbb{C}$, describes the channel coefficient between UE k in cell j and the m-th antenna of the BS in cell b.

Owing to the mobility of the UEs and a changing propagation environment, the channel coefficients will vary with time and they have to be estimated frequently. We assume a frequency-flat block fading channel, where the channel is constant during one block consisting of a coherence interval of C symbols, called the *frame*. We divide each frame into three parts - the training phase, the uplink data phase and the downlink data phase.

Our goal is to evaluate the performance of different channel estimation techniques in the uplink. The uplink signal received at the BS in cell b can be described as

$$\boldsymbol{Y} = \sum_{j=1}^{B} \boldsymbol{H}_{bj}\boldsymbol{X}_j + \boldsymbol{N}, \tag{1}$$

where $\boldsymbol{X}_j \in \mathbb{C}^{K\times L}$ describes the L symbols transmitted by the UEs in cell j and $\boldsymbol{N} \in \mathbb{C}^{M\times L}$ denotes the additive noise whose elements are drawn from a circularly-symmetric complex Normal distribution with zero mean and element-wise variance σ^2.

III. Channel Models for Massive MIMO systems

In this section, we provide a brief overview of the different channel models employed for the evaluation of massive MIMO systems. We determine the best suited model for evaluation based on its computational complexity and its proximity towards the channels obtained from the measurement campaign in [3].

A. Overview of Channel Models

1) Clarke's Model: A widely used model for the analysis of massive MIMO systems is Clarke's model, which is based on the assumption that the propagation environment contains a certain number of scatterers [7]. This model incorporates only the temporal correlation aspect. Since spatial correlation is not included in this model, as the number of scatterers increases, the distribution of the channel coefficients across the antennas will be similar to that of the Rayleigh i.i.d. model.

2) Correlated Rayleigh Model: This model generates the channel coefficients by incorporating the spatial and temporal correlation parameters to the Rayleigh model, while keeping the model's complexity low. One such correlated Rayleigh model is described in [4], which captures the spatial correlation across the BS antennas. In practical scenarios, the number of scatterers in the propagation environment is limited and the signals from different UEs traverse through the same scatterers, resulting in significant spatial correlation across the UEs. Therefore, we extend the model in [4] to capture this aspect.

Similar to [4], our model assumes that the channel at frame t, $\boldsymbol{h}_{bj_kt}$, follows a Gauss-Markov distribution according to

$$\begin{aligned} \boldsymbol{h}_{bj_k0} &= \boldsymbol{R}_{\mathrm{BS}}^{1/2}\boldsymbol{g}_{bj_k0}\boldsymbol{R}_{\mathrm{UE}}^{1/2}, \\ \boldsymbol{h}_{bj_kt} &= \eta\boldsymbol{h}_{bj_k(t-1)} + \sqrt{1-\eta^2}\boldsymbol{R}_{\mathrm{BS}}^{1/2}\boldsymbol{g}_{bj_kt}\boldsymbol{R}_{\mathrm{UE}}^{1/2},\ t \geq 1, \end{aligned} \tag{2}$$

where $\boldsymbol{R}_{\mathrm{BS}} = \mathbb{E}(\boldsymbol{h}_{bj_kt}\boldsymbol{h}_{bj_kt}^H)$ is the spatial correlation matrix across the antennas, following an exponential model given by

$$\boldsymbol{R}_{\mathrm{BS}} = \begin{pmatrix} 1 & a^{\sqrt[M]{1^2}} & \dots & a^{\sqrt[M]{(M-1)^2}} \\ a^{\sqrt[M]{1^2}} & 1 & & \\ \vdots & & \ddots & \\ a^{\sqrt[M]{(M-1)^2}} & & & 1 \end{pmatrix}, \tag{3}$$

where $0 < a < 1$ is a real number. The vector $\boldsymbol{g}_{bj_kt}$ is an innovation process with i.i.d. entries distributed according to $\mathcal{CN}(\boldsymbol{0}, \boldsymbol{I}_M)\ \forall t$, η is a temporal correlation coefficient with $0 \leq \eta \leq 1$ (similar to [4]) and $\boldsymbol{R}_{\mathrm{UE}}$ is the UE spatial correlation matrix given by

$$\boldsymbol{R}_{\mathrm{UE}} = \begin{pmatrix} 1 & b^{(1^2)} & \dots & b^{((K-1)^2)} \\ b^{(1^2)} & 1 & & \\ \vdots & & \ddots & \\ b^{((K-1)^2)} & & & 1 \end{pmatrix}, \tag{4}$$

where $0 < b < 1$ is a real number. Both $\boldsymbol{R}_{\mathrm{BS}}$ and $\boldsymbol{R}_{\mathrm{UE}}$ have the structure of a Toeplitz matrix.

The standard Rayleigh model with i.i.d. spatial and temporal correlation is a special case of this model with $\eta = 0$ and $\boldsymbol{R}_{\mathrm{BS}} = \boldsymbol{I}_M$ and $\boldsymbol{R}_{\mathrm{UE}} = \boldsymbol{I}_K$, where $\boldsymbol{I}_q$ is the $q \times q$ identity matrix.

3) COST 2100 Model: The COST 2100 channel model is a geometry-based stochastic model [3], [11], using cluster-level modelling [6]. The clusters represent the scatterers (e.g. a high-rise building) in the real propagation environment and consist of a package of multiple multi-path components with similar properties. The key idea is that, depending on the location of the UEs, only certain clusters contribute to the propagation of the respective UEs. This approach inherently enables the simulation of multi-user systems and the channel coefficients between the UE and the BS are obtained by superposing all multi-path components of the clusters which are visible at the UE's location. A detailed description of the model can be found in [5] and [6]. The entire process of generating the channel coefficients is computationally intensive since each multi-path link and its associated parameters (pathloss, shadow fading, etc.) has to be separately calculated and the number of such links can be very large.

B. Comparison of Channel Models

In the following, we compare the aforementioned channel models with respect to the joint spatial correlation in the system, which is an important parameter to analyze the propagation conditions in massive MIMO systems [2], [12]. The joint spatial correlation, denoted by κ, is quantified using the condition number or the singular value spread (SVD spread), which is the ratio of the maximum singular value to the minimum singular value of the $M \times K$ channel matrix. If $\kappa = 1$, the channels of the UEs are orthogonal, consequently they are perfectly separable. On the other hand, if the SVD spread is large, at least two of the UEs are not well separable.

The measurement campaign [3] shows that the channels obtained by a slightly modified COST 2100 model reflect

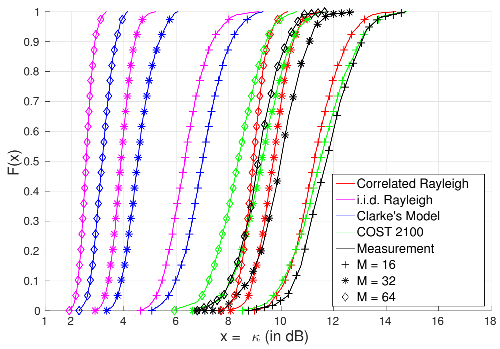

Fig. 1. CDF of the SVD spread of the channels for $K = 9$ active UEs for different channel models

real propagation environments rather well. However, in this work, we use the original COST 2100 model designed for a semi-urban micro cell with cell-radius 500m and non-line-of-sight (NLOS) conditions in our simulations, since not all the modifications have been published yet. The bandwidth of the channel is set to 20 MHz and the UEs are placed in an outdoor environment.

For the correlated Rayleigh model, we set $\eta = 0.95, a = 0.3$ and $b = 0.6$ so that the SVD spread of the channels approximate the practical observations in [3]. The parameters a and b were derived through a grid search such that the Kullback-Leibler divergence between the SVD spread from the measurement campaign in [3] and that generated using our correlated Rayleigh model is minimized. To search for a, we used the range $0 \leq a \leq 0.4$, so that antenna correlation at the BS is relatively low (which in practice can be achieved by suitably choosing the antenna elements and their spacing) and to determine b, we explored the full range of UE correlation values, i.e., $0 \leq b \leq 1$.

Fig. 1 shows the cumulative distribution function (CDF) of the SVD spread of the channels for a system consisting of $K = 9$ UEs per cell. First, we can observe that the channel hardening effect (the CDF becomes steeper with an increasing number of antennas) occurs in all the models. However, the mean value of κ is much smaller for the Rayleigh i.i.d. and Clarke's models, which means that these models provide a smaller correlation among the channels of the UEs than that found in reality. In contrast to this, the correlated Rayleigh and the COST 2100 models approximate the SVD spread obtained in the measurement campaign [3] much better. The COST 2100 model is computationally intensive, while the correlated Rayleigh model requires only two parameters to be tuned - a and b, the spatial correlation parameters to approximate the SVD spread. This makes it a convenient analytical model reflecting real propagation environments more accurately.

IV. Channel Estimation Techniques

In this section, we briefly introduce selected channel estimation techniques for massive MIMO systems. We will investigate two approaches derived from the perspective of pilot contamination and a reduced-complexity approximation of the minimum mean-square error (MMSE) estimator. The MMSE estimator and its approximation assume that the covariance matrix of the channels is available at the BS and use it for channel estimation. Considering that we have M antennas at the BS and K UEs, the covariance matrix of the channels of the UEs of the j-th cell to the BS in the b -th cell is given by

$$\boldsymbol{R}_{bj} = \mathbb{E}\{\tilde{\boldsymbol{h}}_{bj}\tilde{\boldsymbol{h}}_{bj}^{H}\} \in \mathbb{C}^{MK \times MK} \tag{5}$$

where $\tilde{\boldsymbol{h}}_{bj}$ is the vectorized form of $\boldsymbol{H}_{bj}$.

A. Pilot Sequence Hopping and Kalman Filtering

First we consider a channel estimation technique which reduces the effect of pilot contamination, but does not require the covariance matrices of the channels at the BS. In this mechanism, the pilot patterns are randomly assigned to the UEs in each frame and a Kalman filter is then used to track the time-varying channel [7]. The method is designed with the assumption that the channels of different UEs are uncorrelated in the massive MIMO regime and the random pilot assignment de-correlates the contaminating signal across succeeding frames.

To illustrate this mechanism, we follow [7] and consider the estimation of only one scalar channel coefficient. Let us assume that BS b estimates the channel coefficient between UE k of cell b and its m-th antenna, i.e., the m-th entry of $\boldsymbol{h}_{bb_k}$ denoted as $h_{b_m b_k}$. First, the BS correlates the signal received at antenna m, $\boldsymbol{y}^{\mathrm{p}}_{b_m t}$ with the pilot sequence $\boldsymbol{p}_{b_k t}$ of UE k. This removes the undesired signal of all UEs applying a pilot sequence different to $\boldsymbol{p}_{b_k t}$ due to the orthogonality of the sequences. We can thus describe the received signal concerning the k-th UE, at a given time t, as

$$\boldsymbol{y}^{\mathrm{p}}_{b_m k} = h_{b_m b_k}\boldsymbol{p}_{b_k} + \sum_{j,l \in \mathcal{C}_{b_k}} h_{b_m j_l}\boldsymbol{p}_{b_k} + \boldsymbol{n}_{b_m k}, \tag{6}$$

where $\mathcal{C}_{b_k}$ denotes the set of all pairs j, l, identifying all UEs applying the same pilot sequence in the t-th time slot as UE k in cell b and the vector $\boldsymbol{n}_{b_m k}$ denotes the thermal noise received at BS b during the training phase in time slot t.

In the pilot sequence hopping part of this technique, the contaminating signal (the sum in (6)) across consecutive frames is de-correlated by randomly assigning pilot sequences to each UE in each frame. This ensures that the same pilot sequence is combined with different (in best case uncorrelated) channel impulse responses during different frames. The second part of the proposed approach tracks the time-varying channel via a modified Kalman filter. The details of the Kalman filter are provided in [7].

B. Amplitude and Angular Projection

The second method considered in this work is based on the blind pilot decontamination technique described in [8]. In this method, the BS first performs an eigen decomposition of the data received in cell b, $\boldsymbol{Y}^{\mathrm{d}}_{b}$, during the uplink data transmission phase:

$$\boldsymbol{Y}^{\mathrm{d}}_{b}\boldsymbol{Y}^{\mathrm{d}H}_{b} = \boldsymbol{U}_b\boldsymbol{\Lambda}_b\boldsymbol{U}_b^{H}, \tag{7}$$

where $\boldsymbol{U}_b \in \mathbb{C}^{M \times M}$ is a unitary matrix and $\boldsymbol{\Lambda}_b$ is a diagonal matrix whose entries are sorted in non-increasing order. The first K columns of $\boldsymbol{U}_b$, combined in the matrix

$\boldsymbol{E}_b = (\boldsymbol{u}_{b_1}, \boldsymbol{u}_{b_2}, \ldots, \boldsymbol{u}_{b_K}) \in \mathbb{C}^{M \times K}$, form an orthogonal basis of the estimated channel subspace $\boldsymbol{H}_{bb}$. Then, the signal received during the pilot transmission phase, $\boldsymbol{Y}_b^{\mathrm{p}}$, is projected onto the subspace spanned by $\boldsymbol{E}_b$. The channel estimate of the channels describing the propagation of the UEs from the b-th cell to the BS in the b-th cell is then given by

$$\hat{\boldsymbol{H}}_{bb}^{\mathrm{AM}} = \boldsymbol{E}_b \boldsymbol{E}_b^H \boldsymbol{Y}_b^{\mathrm{p}} \boldsymbol{P}_b^H, \tag{8}$$

where $\boldsymbol{P}_b \in \mathbb{C}^{K \times \tau}$ is the pilot transmission matrix with each row containing the pilot sequences of length τ.

An extension of the blind decontamination method is presented in [9]. This approach improves the estimate obtained via (8) by filtering it in the frequency domain. If the channel has a finite angular support, the frequency spectra of the channel power is clustered within a certain frequency range. Consequently, if the channels of the UEs have disjoint angular supports, the powers of the channel of interest and the interfering channels are concentrated in different frequency ranges. This fact is exploited to design a Fourier matrix filtering out all undesired frequency components which do not belong to the UE of interest. This approach is presented in more detail in [9].

C. Polynomial Expansion

The last approach we consider here is based on the MMSE estimator exploiting the covariance matrices of the channels, which are assumed to be available at the BS. The MMSE estimator [10] is given by

$$\hat{\boldsymbol{h}}_{bb}^{\mathrm{MMSE}} = \boldsymbol{R}_{bb} \overline{\boldsymbol{P}}_b^H \left(\overline{\boldsymbol{P}}_b \boldsymbol{R}_{bb} \overline{\boldsymbol{P}}_b^H + \boldsymbol{S}_b \right)^{-1} \boldsymbol{y}_b^{\mathrm{p}}, \tag{9}$$

where $\boldsymbol{y}_b^{\mathrm{p}} = \mathrm{vec}(\boldsymbol{Y}_b^{\mathrm{p}})$ is the vectorized form of the receive matrix during the training phase, $\overline{\boldsymbol{P}}_j = \boldsymbol{P}_j^T \otimes \boldsymbol{I}_M$ and $\boldsymbol{R}_{bj}$ is the covariance matrix defined in (5) and $\tilde{\boldsymbol{h}}_{bj} = \mathrm{vec}(\boldsymbol{H}_{bj})$. The covariance matrix of the contaminating signal is given as

$$\boldsymbol{S}_b = \sum_{j=1, j \neq b}^{B} \overline{\boldsymbol{P}}_j \boldsymbol{R}_{bj} \overline{\boldsymbol{P}}_j^H + \boldsymbol{N_b}. \tag{10}$$

In order to reduce the complexity of the MMSE receiver, [10] proposes three different approaches. We will consider two of them in the sequel. The simplest approach is to diagonalize the covariance matrices, i.e., we set all off-diagonal elements to zero. This reduces the computational complexity significantly since $\overline{\boldsymbol{P}}_b \boldsymbol{R}_{bb} \overline{\boldsymbol{P}}_b^H + \boldsymbol{S}_b$ is then a diagonal matrix which can be inverted easily. The diagonalized estimator is given as

$$\hat{\boldsymbol{h}}_{bb}^{\mathrm{diag}} = \boldsymbol{R}_{bb}^{\mathrm{diag}} \overline{\boldsymbol{P}}_b^H \left(\overline{\boldsymbol{P}}_b \boldsymbol{R}_{bb}^{\mathrm{diag}} \overline{\boldsymbol{P}}_b^H + \boldsymbol{S}_b^{\mathrm{diag}} \right)^{-1} \boldsymbol{y}_b^{\mathrm{p}}, \tag{11}$$

where $\boldsymbol{R}_{bb}^{\mathrm{diag}}$ and $\boldsymbol{S}_b^{\mathrm{diag}}$ are obtained by setting all off-diagonal elements of $\boldsymbol{R}_{bb}$ and $\boldsymbol{S}_b$ to zero.

Another approach to reduce the complexity of the estimator is to compute the inverse appearing in (9) by means of an L-degree polynomial approximation. This leads to the so-called *PEACH* estimator [10]:

$$\hat{\boldsymbol{h}}_{bb}^{\mathrm{PEACH}} = \boldsymbol{R}_{bb} \overline{\boldsymbol{P}}_b^H \sum_{l=0}^{L} \alpha (\boldsymbol{I}_{M\tau_p} - \alpha(\overline{\boldsymbol{P}}_b \boldsymbol{R}_{bb} \overline{\boldsymbol{P}}_b^H + \boldsymbol{S}_b))^l \boldsymbol{y}_b^{\mathrm{p}}, \tag{12}$$

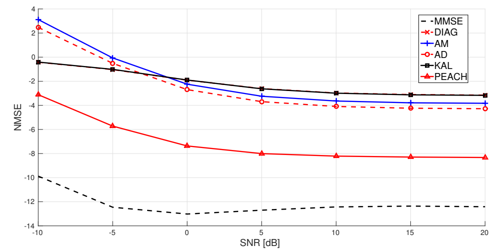

(a) Clarke's multi-path model

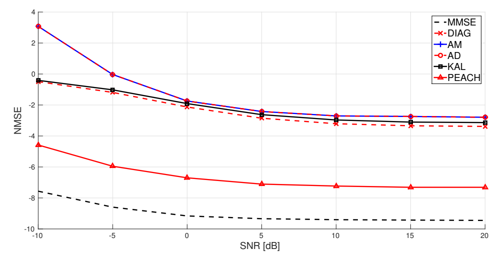

(b) Correlated Rayleigh model

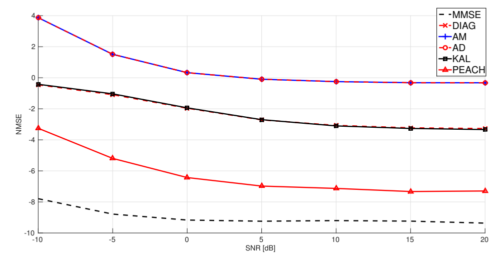

(c) COST 2100 model

Fig. 2. Performance of channel estimation techniques under the presence of pilot contamination.

where τ_p is the length of the pilot sequences and the weighting factor is given by $\alpha^{-1} = \mathrm{tr}\left(\overline{\boldsymbol{P}}_b \boldsymbol{R}_{bb} \overline{\boldsymbol{P}}_b^H + \boldsymbol{S}_b \right)/2$.

V. Simulation Results

In this section, we evaluate the performance of the channel estimation techniques discussed in Section IV using the correlated Rayleigh Model and the COST 2100 model, since these models align well with the realistic scenarios for massive MIMO. We use $B = 7$ cells, $M = 64$ antennas per BS and all cells contain the same number of active UEs (K), set to 9. Each cell uses the same set of K orthogonal pilot patterns. We adopt the identity matrix as a basis pilot matrix and consider the case that the interfering signals are as strong as the signal of interest, i.e., SIR $= 0$ dB similar to [10]. As an indicator of the performance measure, we use the normalized mean squared error (NMSE), defined as

$$\mathrm{NMSE} = 10 \log_{10} \left(\frac{1}{K} \sum_{k=1}^{K} \frac{\|\hat{\boldsymbol{h}}_{bb_k} - \boldsymbol{h}_{bb_k}\|^2}{\|\boldsymbol{h}_{bb_k}\|^2} \right), \tag{13}$$

where $\boldsymbol{h}_{bb_k}$ is the actual channel of UE k of cell b to the BS in cell b and $\hat{\boldsymbol{h}}_{bb_k}$ is its estimate.

In the following, the diagonal estimator, Kalman filtering technique, the amplitude and angular based techniques are identified as "DIAG", "KAL", "AM" and "AD" respectively.

Some estimation techniques require a time-varying channel, therefore we assumed that the channel evolves over 20 training phases and set the time between two training phases to 1ms. The parameters used for the channel estimation techniques are the same as that in the original work, except for the AD estimator, where the averaging was done using 10 channel estimates.

Fig. 2a, Fig. 2b and Fig. 2c depict the performance of the different channel estimation techniques for Clarke's multipath model, the correlated Rayleigh model and the COST 2100 model respectively. A lower value of NMSE indicates better performance. We see that all the channel estimation techniques considered in this work show similar behaviour for the correlated Rayleigh and COST 2100 models, indicating that the correlated Rayleigh model can be used as a viable alternative for the performance evaluation of channel estimation techniques in massive MIMO.

We observe that the performance of the blind method (AM) and its extension (AD) is slightly degraded for the correlated Rayleigh and the COST 2100 models, when compared to Clarke's model, because of the spatial correlation in these channel models. In particular, for SNR $>$ 0 dB, the AM technique is degraded by about 0.5 dB to 1 dB for the correlated Rayleigh model and by about 2 dB to 3.5 dB for COST 2100 model, when compared to Clarke's model. The corresponding degradation for the AD technique is 1 dB to 1.3 dB for the correlated Rayleigh model and 2.5 dB to 4 dB for COST 2100 model. The small difference in the amount of degradation between the correlated Rayleigh and COST 2100 models is because their SVD spreads are similar, but not identical (see Fig. 1).

Also, the AD technique, which shows an improved performance for Clarke's model for small values of M in [9], shows minimal improvement for $M = 64$. This behaviour can be explained by investigating the channel power spectrum of the UEs in more detail. In Clarke's model, the UEs can be separated by their channel powers in the frequency domain pretty well. In fact, the power of the individual UE channels is clustered in different frequency ranges, thereby enabling improved cancellation of signals of the UEs. However, the presence of spatial correlation in practical channels reduces the extent of channel power clustering. Therefore, the AD technique does not provide any improvement over the AM technique for the correlated Rayleigh and COST 2100 models as indicated in Fig. 2b and Fig. 2c respectively.

The KAL technique performs almost identically under all the models. This can be explained by the fact that only the pilot sequence hopping strategy involved in this estimator requires uncorrelated channels, while the Kalman filter works for both correlated and uncorrelated channels as long as it knows the total contamination power. Since the simulations were performed with only 9 UEs, the effect of pilot sequence hopping is minimal and the KAL technique shows identical performance for all the models. The performance of the DIAG estimator is similar to that of the KAL technique.

The MMSE and the PEACH estimators provide the best performance under all the channel models. This is intuitively clear, since these estimators are the only ones exploiting knowledge about the covariance matrices of the channel of interest and the interfering channels. Moreover, we can improve the performance of the PEACH estimator by increasing the degree of the polynomial approximating the inverse of the covariance matrix.

VI. Conclusion

In this work, we examined the effect of the underlying channel model on the performance of massive MIMO systems. We observed that the COST 2100 and the correlated Rayleigh models, incorporating the spatial correlation parameters serve as a good approximation for massive MIMO channels, with the latter being more convenient for analysis owing to its lower computational complexity. Then, we evaluated the performance of selected channel estimation techniques for different channel models. We discovered that the blind channel estimation techniques of amplitude and angular based projection are more sensitive to the underlying channel model and show a small degradation in performance for the aforementioned channel models with spatial correlation, when compared to Clarke's model. We demonstrated that Kalman filter based technique and the diagonal estimator show similar performance for all the channel models, while the polynomial expansion estimator shows the best performance.

References

[1] E. Larsson, O. Edfors, F. Tufvesson, and T. Marzetta, "Massive mimo for next generation wireless systems," *IEEE Commun. Mag.*, vol. 52, no. 2, pp. 186–195, 2014.

[2] F. Rusek, D. Persson, B. K. Lau, E. Larsson, T. Marzetta, O. Edfors, and F. Tufvesson, "Scaling Up MIMO: Opportunities and Challenges with Very Large Arrays," *IEEE Signal Process. Mag.*, vol. 30, no. 1, pp. 40–60, Jan 2013.

[3] O. Edfors and F. Tufvesson, "D1.2 MaMi Channel Characteristics: Measurement Results," Jul 2015.

[4] J. Choi, D. Love, and P. Bidigare, "Downlink Training Techniques for FDD Massive MIMO Systems: Open-Loop and Closed-Loop Training With Memory," *IEEE J. Sel. Topics Signal Process.*, vol. 8, no. 5, pp. 802–814, Oct 2014.

[5] J. Poutanen, "Geometry-based radio channel modeling: Propagation analysis and concept development," PhD Thesis, Aalto University, 2011.

[6] L. Liu, C. Oestges, J. Poutanen, K. Haneda, P. Vainikainen, F. Quitin, F. Tufvesson, and P. Doncker, "The COST 2100 MIMO channel model," *IEEE Wireless Commun.*, vol. 19, no. 6, pp. 92–99, Dec 2012.

[7] J. Sorensen and E. de Carvalho, "Pilot decontamination through pilot sequence hopping in massive MIMO systems," in *Proc. IEEE Global Commun. Conf.*, 2014, pp. 3285–3290.

[8] R. Müller, L. Cottatellucci, and M. Vehkapera, "Blind Pilot Decontamination," *IEEE J. Sel. Topics Signal Process.*, vol. 8, no. 5, pp. 773–786, 2014.

[9] H. Yin, L. Cottatellucci, D. Gesbert, R. Müller, and G. He, "Pilot decontamination using combined angular and amplitude based projections in massive MIMO systems," in *Proc. IEEE 8th Wkshp. on Signal Process. Advances in Wireless Commun.*, Stockholm, SWEDEN, Jun 2015.

[10] N. Shariati, E. Björnson, M. Bengtsson, and M. Debbah, "Low-complexity polynomial channel estimation in large-scale MIMO with arbitrary statistics," *IEEE J. Sel. Topics Signal Process.*, vol. 8, no. 5, pp. 815–830, 2014.

[11] X. Gao, F. Tufvesson, and O. Edfors, "Massive MIMO channels - Measurements and models," in *Asilomar Conf. on Signals, Syst. and Comput.*, Nov 2013, pp. 280–284.

[12] J. Hoydis, C. Hoek, T. Wild, and S. ten Brink, "Channel measurements for large antenna arrays," in *Proc. Int. Symp. on Wireless Commun. Sys.*, Aug 2012, pp. 811–815.